

Deconvolution of X-ray Diffraction Data To Elucidate Plastic Deformation Mechanisms in the Uniaxial Extension of Bulk Nylon 6

A. Galeski

Centre of Molecular and Macromolecular Studies, Polish Academy of Sciences, 90-362 Lodz, Poland

A. S. Argon and R. E. Cohen*

Massachusetts Institute of Technology, Cambridge, Massachusetts 02139

Received September 20, 1990; Revised Manuscript Received February 18, 1991

ABSTRACT: A least-square peak deconvolution procedure was applied to wide-angle X-ray diffraction data on uniaxially drawn nylon 6 so that pole figures could be generated from clearly separated crystallographic reflections. Beside peak total intensity pole figures a new type of pole figure, based on peak widths, was proposed and proved to be useful in elucidating the mechanisms of plastic deformation in the nylon 6 samples. In uniaxial tension α and γ crystals of nylon 6 become oriented with macromolecular chains parallel to the drawing direction. In contrast to γ crystals, α crystals experience a large amount of breakdown between planes containing hydrogen bonds. Macromolecules that are in the amorphous phases are mostly aligned along the drawing direction and that fraction of the amorphous phase that is so oriented shows the smallest peak width.

I. Introduction

The development of powerful sources of X-ray radiation and computer-aided data collection has greatly increased the possibility of more precise characterization of molecular orientation and molecular order by X-ray diffraction experiments. In order to describe the orientation of crystallographic axes of crystallites in a polycrystalline sample a three-dimensional coordinate system is introduced. For example, to describe the texture of rolled sheets, coordinate axes have been defined along the machine direction (MD), transverse direction (TD), and normal direction (ND.) The orientation of a unit vector normal to a given crystallographic plane can then be described by two angles α and β where, α is the angle between machine direction and the normal and β is the angle between the projection of that normal on the ND-TD plane and TD direction. Pole figures provide a convenient way to represent a map of the orientation distribution function of the normals to any selected crystallographic plane (e.g., ref 1).

Intensities for pole figure level contours are generally obtained on an X-ray diffractometer in the following manner. The position of the detector is set at the 2θ angle corresponding to a selected (hkl) reflection, while the sample assumes all possible orientations $0 < \alpha < 90^\circ$ and $0 < \beta < 360^\circ$. In the case of polymeric materials, the crystals are so small that all reflections show considerable broadening, overlapping over each other; a very broad amorphous halo also underlies most of the crystallographic reflections. In order to deconvolute overlapping peaks, pole figure intensity data must be collected over the entire range of 2θ angles for which crystallographic reflections occur. This extremely time-consuming task is not usually performed, although one recent example has appeared in the literature² for the case of poly(ethylene terephthalate). The use of powerful X-ray sources and the application of computer-aided data collection reduce the duration of the measurements and the data processing to an acceptable level.

The data obtained after deconvolution of overlapping peaks contain information about the heights and widths

of peaks. The total peak intensity, the area under each deconvoluted peak, must be used for correct pole figure construction. In addition, we suggest in the present paper that the construction of another type of pole figure, based on peak widths, is also useful for gaining an understanding of morphological details in deformed semicrystalline polymers. A peak width depends upon the size of the crystals in the direction normal to a given diffraction plane and upon the deformation of crystallographic units due to frozen stresses. We demonstrate here that the analysis of pairs of pole figures, constructed from total peak intensities and from peak widths, provides valuable information about the mechanisms of plastic deformation of crystals in semicrystalline polymers.

For this study we have chosen polyamide 6 bulk samples, which we have previously carefully characterized in terms of their undeformed bulk morphology.³ These same materials have been examined also by transmission electron microscopy to obtain a qualitative sense of evolution of morphological change that accompanies plastic deformation in uniaxial tension.⁴

II. Materials and Methods

Polyamide 6 (Capron 8200 extracted, Allied Corp.) was the material used in this work. Size-exclusion chromatography experiments using trifluoroethanol as a mobile phase revealed a weight-average molecular weight M_w of 32.6 kg/mol and a polydispersity index, M_w/M_n , of 1.80 for Capron 8200. Plaques of 3-mm thickness were obtained by compression molding and by injection molding; the cooling cycle was considerably faster for the injection molding process. The outer layers of the plaques were removed by machining at room temperature, leaving a 1-mm-thick core. Surfaces of the specimens were rough ground with 800-mesh silicon carbide paper and then carefully polished with 0.3- μ m alumina powder and finally with 0.05- μ m alumina powder. Polished plates were then dried at 100 °C under vacuum for 24 h and stored at 60% relative humidity for 18 months.

Oar-shaped samples for tensile testing were cut out from machined cores of plaques; the gauge length of specimens was 18 mm and the width was 16 mm. The uniaxial extension of the samples was performed on a Model 1122 Instron tensile testing machine at a rate of 1 mm/min. The drawing was interrupted at an engineering strain of 2.5 and the samples were allowed to

Table I
Initial Values (Radians) for Peak Width and Position

		α form		γ form	
amorphous		(200)	(002)	(020)	(200)
Injection Molded					
width	0.054 ± 0.017	0.014 ± 0.007	0.012 ± 0.007	0.019 ± 0.007	0.020 ± 0.007
position	0.380 ± 0.0035	0.349 ± 0.0035	0.397 ± 0.0035	0.186 ± 0.0035	0.373 ± 0.0035
Compression Molded					
width	0.058 ± 0.017	0.014 ± 0.007	0.014 ± 0.007	0.019 ± 0.007	0.014 ± 0.007
position	0.378 ± 0.0035	0.353 ± 0.0035	0.398 ± 0.0035	0.190 ± 0.0035	0.374 ± 0.0035

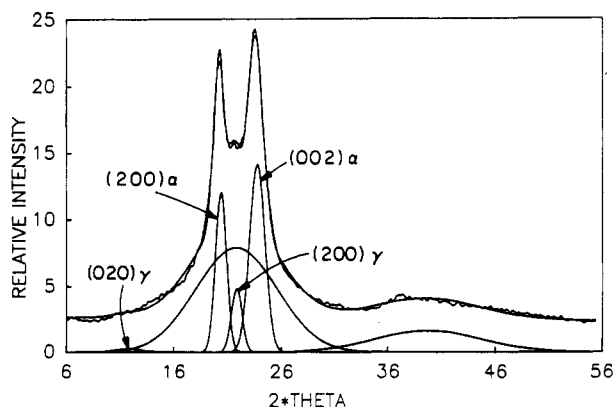


Figure 1. Deconvolution of the X-ray diffraction curve for a nylon 6 compression-molded sample: X-ray diffraction curve, fitting to the experimental curve, and deconvoluted peaks are drawn.

relax under stress for 30 min. The engineering natural draw ratio as determined from the reduction in cross section for injection-molded sample was 2.22, while for compression-molded sample it was 2.16.

The gauge sections of each specimen were examined by means of X-ray diffraction. A typical diffraction pattern for nylon 6 compression-molded sample is presented in Figure 1. For nylon 6 samples there are at least five overlapping peaks of α , γ , and amorphous phases listed in Table I (see Gurato et al.⁵ for comparison). Because of this type of overlap, which is relatively common in polymers, we developed a suitable method of peak deconvolution that relies on a minimization procedure for a least-squares expression. In this expression the peaks were approximated by Gaussian curves $A_i \exp[-(2\theta_i - 2\theta)^2/2\sigma_i^2]$ and the background was subtracted. The minimization procedure searches for the direction of the steepest slope of the above expression and the values A_i/θ_i and σ_i are changed accordingly. The search is performed with a step size of 10% of the assumed range of variability for respective A_i , θ_i , and σ_i parameters.

The set of actual values of A_i , θ_i , and σ_i is systematically changed in the direction of the steepest slope until the minimum is found. At this new point of A_i , θ_i , and σ_i a new direction of the steepest slope is sought. If this direction is not found, then the step is adjusted to 0.8 of the present value and the procedure is repeated. The overall minimization procedure ends when the assumed accuracy in steps for A_i , θ_i , and σ_i is reached, yielding the final fitted values for height, position, and width for all diffraction peaks.

The minimization procedure requires a starting point, i.e., a set of approximate initial values for height, position, and width of peaks. The initial values should be within physically reasonable limits and as close as possible to the actual values. It has been established by comparison of x-ray diffraction curves for deformed and undeformed nylon 6 samples that the values and limits for peak positions and widths for nylon 6 samples provided in Table I are reasonable.

The deconvolution procedure is illustrated in Figure 1 for a compression-molded undeformed sample. The deconvolution of X-ray diffraction revealed crystallinity levels of about 25% α and 13% γ forms in compression-molded samples and 15% α and 28% γ forms in the injection-molded samples.

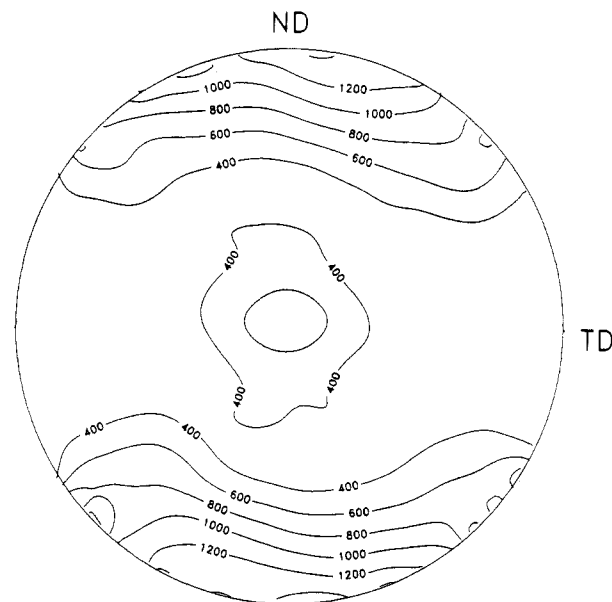


Figure 2. Pole figure of the nondeconvoluted X-ray diffraction intensity integrated over the range $10^\circ < 2\theta < 12^\circ$ for the uniaxially drawn injection-molded nylon 6 sample. Corrections for absorption, polarization, and background are incorporated.

A Rigaku X-ray diffractometer with a rotating anode source was employed throughout the work. The Cu $K\alpha$ radiation generated at 40 kV and 150 mA was filtered by electronic filtering and a thin-film Ni filter. A Rigaku pole figure attachment was controlled on-line, and X-ray diffraction data were collected by means of a Micro VAX computer running under DMAXB Rigaku-USA software. For this study, complete pole figures were obtained for the projection of Euler angles of sample orientation: β from 0° to 360° with steps of 5° , and α in the range 0° to 90° with steps of 5° . X-ray data from the transmission and reflection modes were connected at the angle $\alpha = 40^\circ$.

In order to obtain the correct pole figures for the five most intense nylon 6 peaks, a sequence of pole figures were collected at 2θ diffraction angle covering the range from 8° to 33° with steps of $1/3^\circ$. For each pair of α and β angles the diffraction intensity was taken from the pole figure collected at the appropriate 2θ angle. The diffraction curves were then corrected for absorption and polarization factors. The deconvolution procedure described above was applied to these reconstructed diffraction curves (there were $20 \times 72 = 1440$ respective pairs of α and β Euler angles; hence 1440 diffraction curves for each sample). New pole figures based on total intensities were then constructed for all five peaks including the amorphous peak.

An example of a nondeconvoluted pole figure for the uniaxially drawn injection-molded nylon 6 sample is given in Figure 2. The total X-ray diffraction intensity from the 2θ range 10 – 12° (corrected for absorption, polarization, and background) was used for the construction of the pole figure. Normally at this 2θ range the (020) reflection for the γ form of nylon 6 is expected to be dominant. The corresponding pole figure for the (020) γ -form peak after deconvolution is presented later in this paper in Figure 6c. It is seen that this pole figure shows most of the normals of (020) planes for the γ form to be oriented along the drawing direction, which is a completely different feature from that revealed in Figure 2. This example illustrates dramatically the

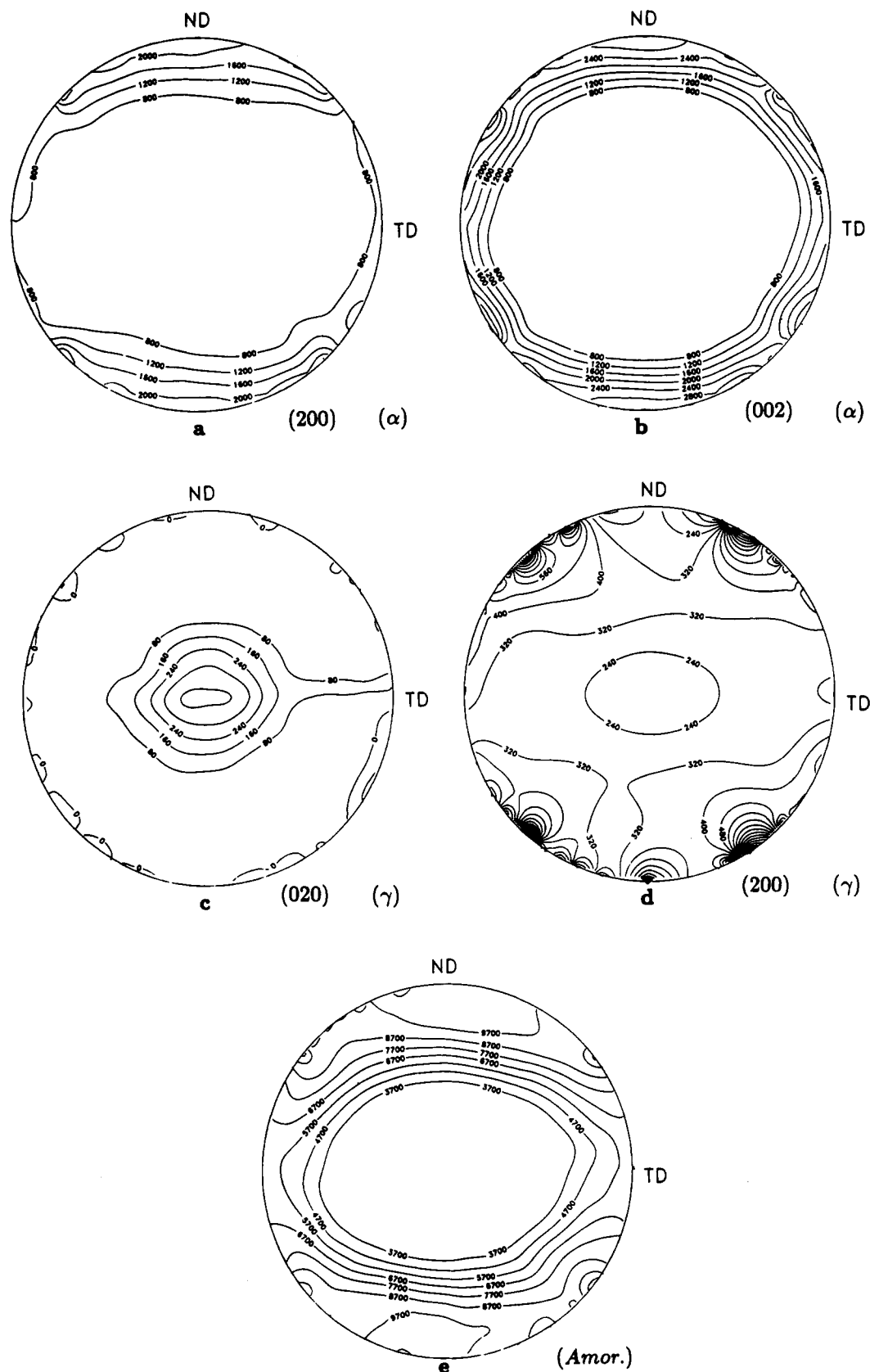


Figure 3. Deconvoluted pole figures for total intensity under the peak for a uniaxially drawn compression-molded sample: (a) (200) plane of the α form; (b) (002) plane of the α form; (c) (020) plane of the γ form; (d) (200) plane of the γ form; (e) amorphous peak.

value of the deconvolution procedure in showing what really occurs during deformation of a sample.

It is also possible to construct a set of pole figures from the data for peak widths. The interpretation of these pole figures is based on the consideration that the plotted value is the X-ray diffraction peak width of that fraction of crystals that is oriented at Euler angles α and β ; the appropriate fraction is taken from

the corresponding total intensity pole figure. It is well established that polycrystalline samples give broad X-ray reflections; the smaller the number of crystallographic planes in crystallites producing diffraction, the broader is the X-ray diffraction peak.⁶ For example, when a crystalline region is reasonably well described by a cubic shape, we can define a quantity δ that relates the peak width and size of the crystals: $\delta = (K\lambda/t) \cos \theta$, where δ is the

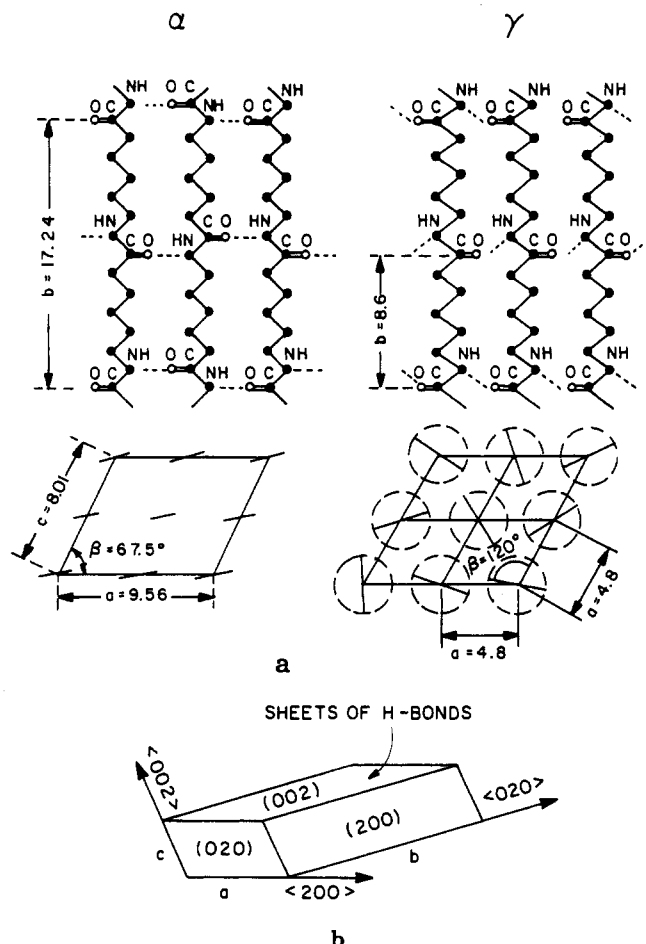


Figure 4. (a) Crystallographic unit cells for the α and γ forms of nylon 6 according to Holmes et al.⁷ (b) Reference unit cell for both types of monoclinic nylon 6.

half-width of the peak, K is a Scherrer constant, λ is the wavelength of X-ray radiation, and t is the dimension of the cube, i.e., the size of the crystal.⁶ The other sources of widening of X-ray diffraction peaks for polycrystalline samples are residual stresses and local defects that cause distortions in a regular crystal structure.⁶ Considering the above relations, the peak width can be treated as a qualitative measure of a mean size of roughly undisturbed crystal structure in the respective (hkl) direction. The pole figure of peak width is in fact a map of X-ray averaged sizes of regions with roughly undisturbed crystal structure.

III. Results and Discussion

Due to the flat shape of samples, the X-ray diffraction intensities for pole figures were acquired in the configuration with the loading direction vertical, the transverse direction horizontal, and the normal direction perpendicular to the plane of a plot. For the purpose of better illustrating the on-going evolution of orientation and deformation of crystallites, the pole figures were projected on the plane with normal direction (ND) vertical and transverse direction (TD) horizontal, i.e., the loading direction coming out of the plane of the plot.

Figure 3a–e shows the pole figures of deconvoluted total intensity for the uniaxially drawn compression-molded sample ($\lambda = 2.16$), in the following order: the (200) α -nylon 6 reflection, the (002) α peak, the (020) γ peak, the (200) γ peak, and the amorphous halo. Figure 3a is the pole figure for the total intensity under the (200) α -form diffraction peak (i.e., the relative fraction of crystals having normals to the (200) plane oriented at angles α and β with respect to the draw direction when the drawing direction is $\alpha = 90^\circ$). Figure 4, drawn after Holmes et al.,⁷ which

will be helpful in further discussion, shows the crystal structure of the α and γ forms of nylon 6. Here we note that the normal to the (200) plane of nylon 6 α and γ crystals is not parallel to the a axis (i.e., (200) direction) and the normal to the (002) plane is not parallel to the c axis (i.e., (002) direction). The X-ray measurements deliver direct data on the orientation of normals to the reflecting crystallographic planes rather than on the orientation of respective (hkl) directions. Also, the reflection peak width contains information about the number of undisturbed crystallographic unit cells along the normals. However, it can be noticed that the number of (200) planes in the (200) direction (a axis) in the crystal is the same as in the direction normal to the (200) plane (albeit not at the same spacing). The same applies to the (002) direction and normal to the (002) plane for nylon 6 α and γ crystals. As seen in the pole figure of Figure 3a, a large fraction of crystals is oriented with the (200) plane parallel to the drawing direction; the (200) normals are perpendicular to the drawing direction—most of them oriented at α angle below 30° —and their β angle is at 90° and 270° fans. A relatively smaller abundance of (200) normals is found at α angles above 30° .

Figure 5 represents the pole figures of peak width for a uniaxially drawn compression-molded ($\lambda = 2.16$) sample for the same series of peaks. It can be determined from Figure 5a, the pole figure for the (200) α -form peak width, that α crystals are only slightly disrupted in the a axis direction over the whole range of α and β angles except for the two regions at the transverse direction fans (TD), where the disruption is even less. The small fraction of a crystallites whose (200) plane normals are oriented around the loading direction (compare Figure 3a) underwent relatively more extensive disruption; the peak half-width reaches more than 0.018.

Pole figures for normals to the (002) planes for α -form nylon 6 are depicted in Figure 3b for total intensity and in Figure 5b for peak width. Most of the α crystals are preferentially oriented with the normal to the (002) plane and also the c axis, perpendicular to the drawing direction. There is a slight asymmetry in orientation around the drawing direction, which probably results from the flat oar-shaped geometry of the sample of 1-mm thickness and 16-mm width. As indicated by the changes in the peak width (Figure 5b), there is a great deal of crystal disruption between (002) planes that contain the sheets of hydrogen bonds; the peak width is about twice that before deformation. This disruption is less pronounced for that small fraction of α crystals (compare Figure 3b) that is oriented with (002) normals around the drawing direction; macromolecular chains in that fraction of α crystals are oriented around the drawing direction as can be deduced from Figure 4.

There is no distinct diffraction peak for planes perpendicular to the macromolecular chains, the b axis, for the α form of nylon 6. The peak for the (0 14 0) plane at $2\theta = 77^\circ$, which is reported in literature (e.g., ref 8), does not appear in our oriented specimens in any readily recognizable form. However, the preferred orientations of the a and c axes, both being perpendicular to the drawing direction, indicate that the majority of α -crystallites is aligned with the b axis along the deformation direction.

The state of orientation of normals to the (200) and (002) planes indicates some discrepancies from pure uniaxial symmetry; also the distributions of peak widths show some departure from symmetry. Similar discrepancies for peak intensity pole figures for some other rolled materials were interpreted by Rober et al.² as tilting of

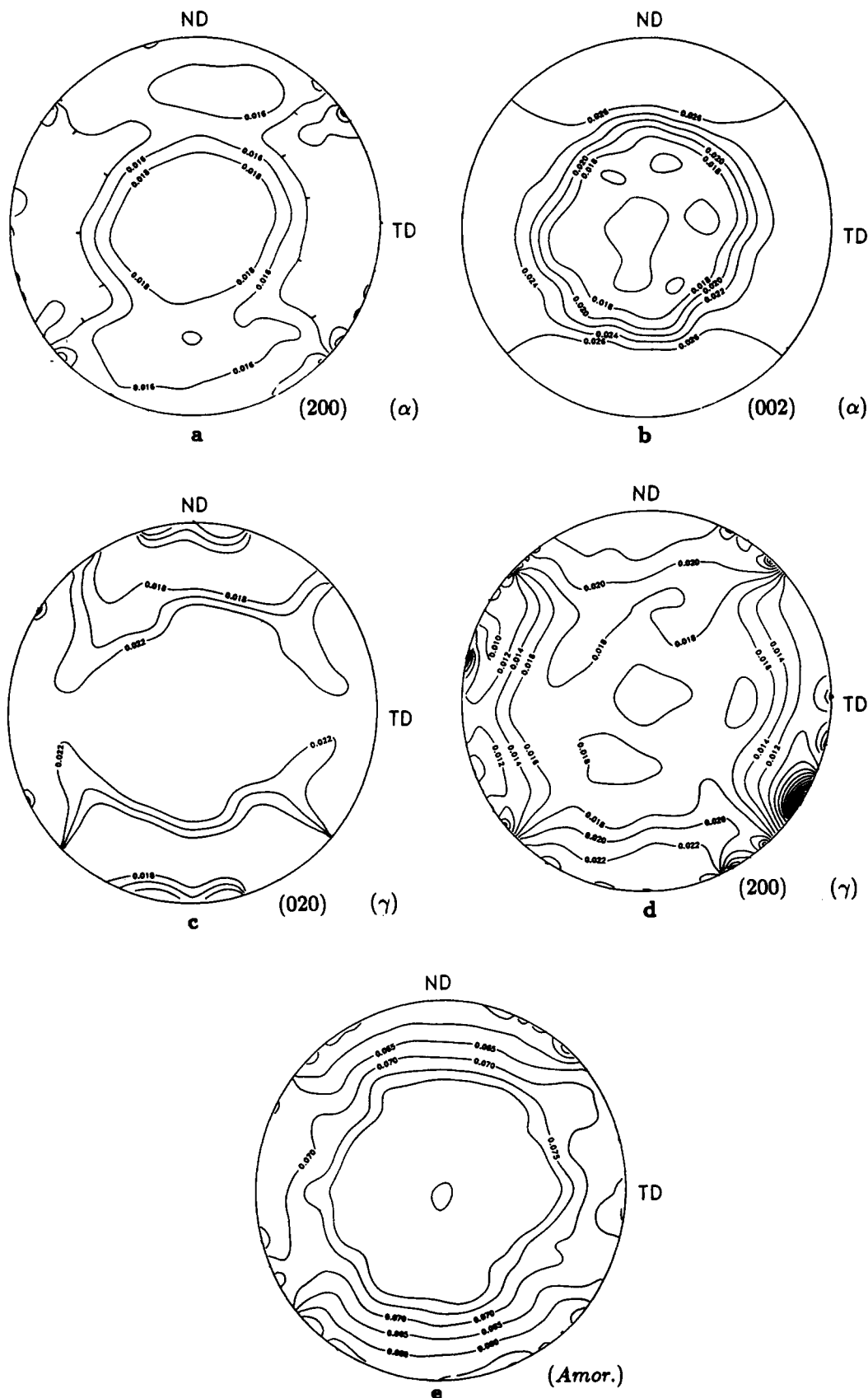


Figure 5. Deconvoluted pole figure for the peak width for a uniaxially drawn compression-molded sample: (a) (200) plane of the α form; (b) (002) plane of the α form; (c) (020) plane of the γ form; (d) (200) plane of the γ form; (e) amorphous peak.

chain axes with respect to the crystal surface. In our case, it is rather more probable that the observed asymmetry in pole figures in Figures 3 and 5 follows from the initial geometry of the tensile samples. Here, the presented data suggest that the slip processes along and across the macromolecular chains in planes containing hydrogen bonds

are active mechanisms that should result in tilting of the chain axis with respect to the crystal surface. However, such tilting, even if it exists, may not be visible in X-ray diffraction intensity and peak width pole figures especially in the absence of (0n0) peak width pole figures for α crystallites. It can be, nevertheless, concluded that disruption

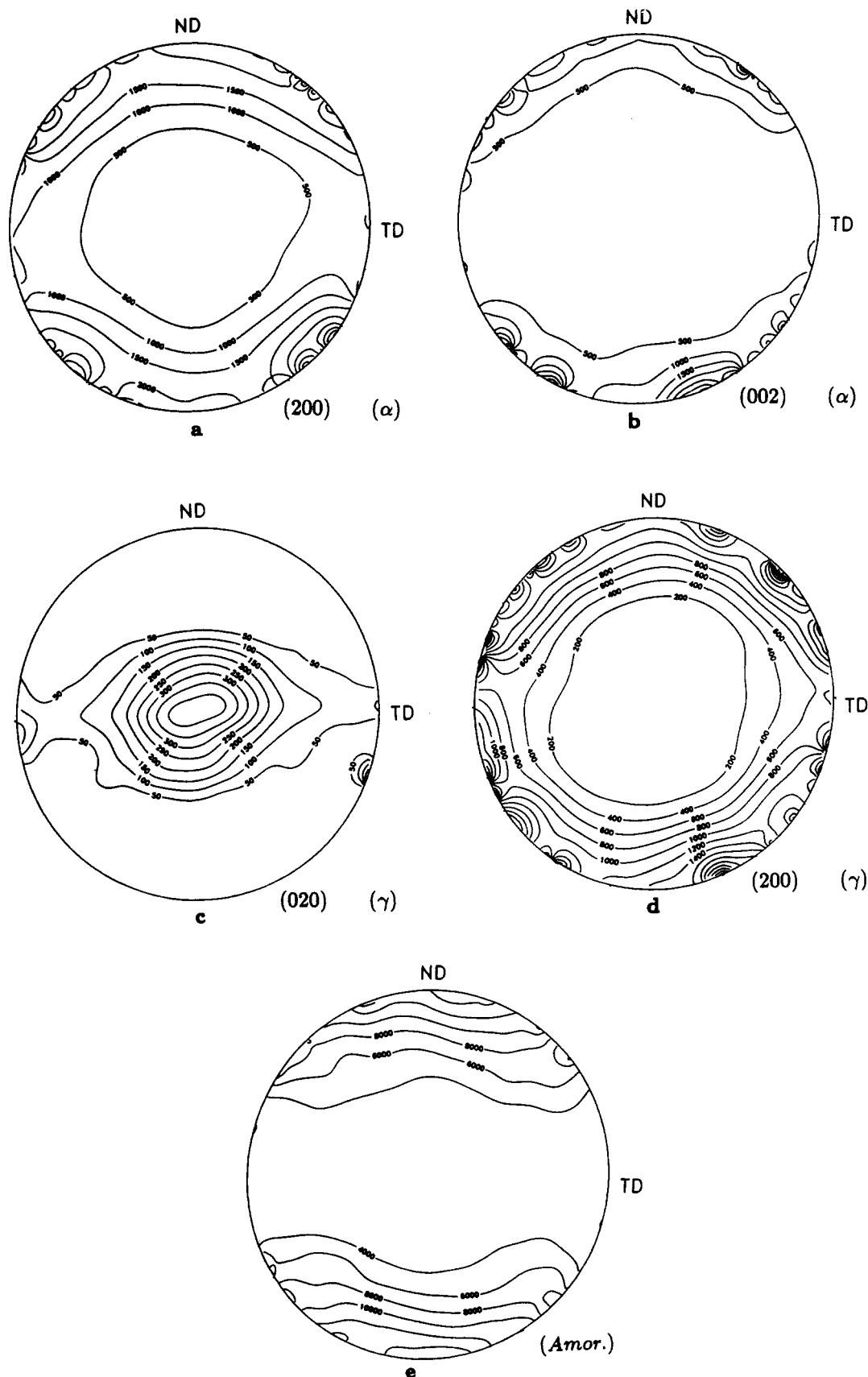


Figure 6. Deconvoluted pole figures for the total intensity under the peak for a uniaxially drawn injection-molded sample: (a) (200) plane of the α form; (b) (002) plane of the α form; (c) (020) plane of the γ form; (d) (200) plane of the γ form; (e) amorphous peak.

of α crystals mostly between (002) planes supports the mechanism of lamellar unravelling proposed by Peterlin.⁹⁻¹¹

The fraction of crystals that exists in the γ form is oriented with the b axis along the deformation direction as is seen from the (020) pole figure in Figure 3c. The

corresponding pole figure for peak width (Figure 5c) shows only a slight change of the crystallites along the b axis. The pole figure for normals to the (200) planes of the γ form is presented in Figure 3d. This pole figure essentially resembles the results obtained for (200) planes of the α

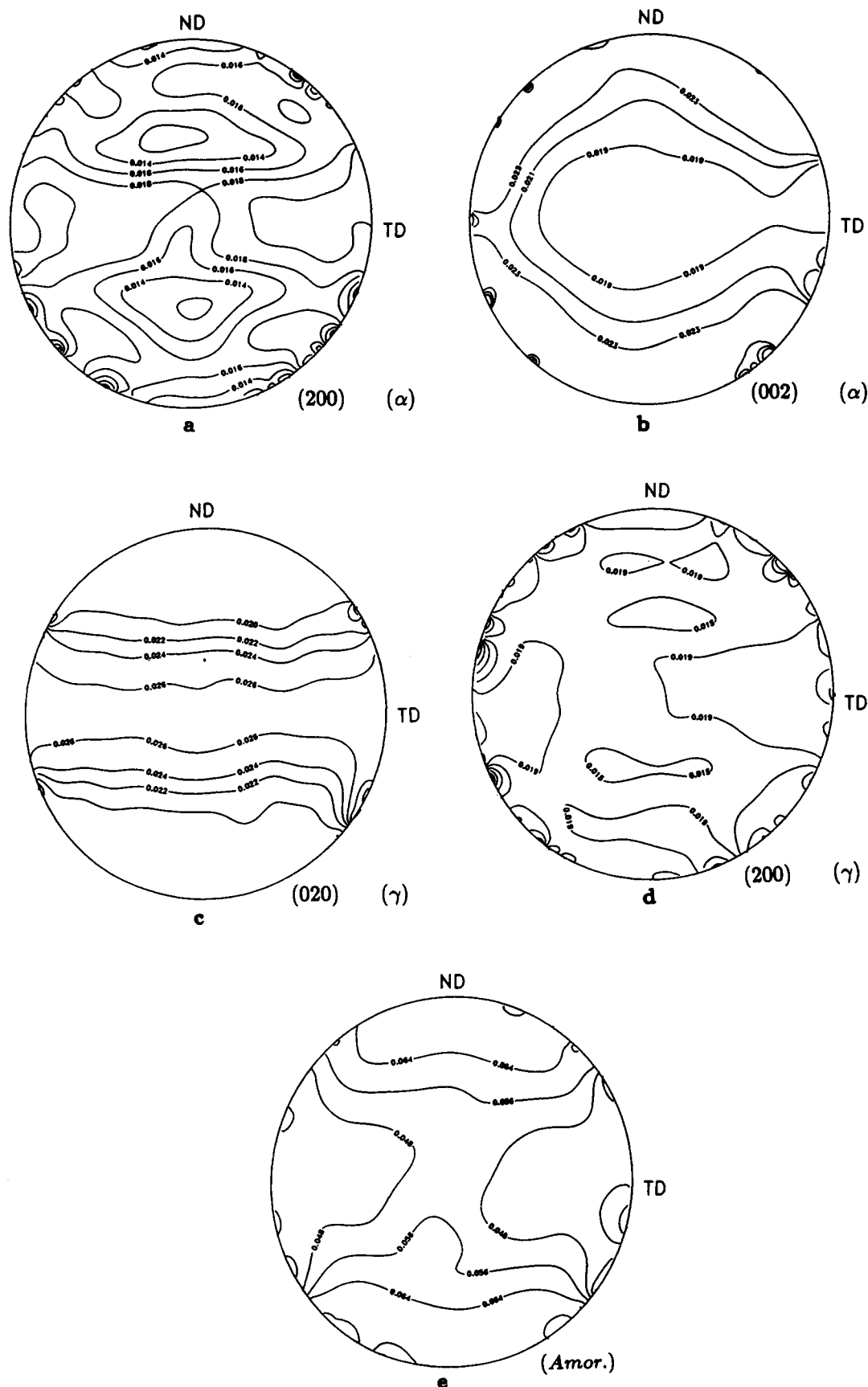


Figure 7. Deconvoluted pole figure for the peak width for a uniaxially drawn injection-molded sample: (a) (200) plane of the α form; (b) (002) plane of the α form; (c) (020) plane of the γ form; (d) (200) plane of the γ form; (e) amorphous peak.

form although one sees much lower total intensity and less defined orientation of (200) γ planes in the direction of drawing. Again the asymmetry seen here is a result of the initial flat shape of the sample. The disruption of γ

crystals along the normal to the (200) plane and also the a axis (see Figure 5d) for the corresponding pole figure of peak width) is not strong and is rather uniform except for the same two regions noted for the (200) plane of α crystals,

i.e., at the transverse direction fans where the disruption is even lower. (Similar conclusions apply for the (002) planes since γ crystals have a hexagonal monoclinic unit cell with axes $a = c$). Lamellar unravelling is not a very intense mechanism for the γ form at this stage of deformation as can be concluded from the relatively small change of (200) peak width in Figure 5d.

The amorphous halo at 2θ in the range 17–23 °C contains information about intermolecular relations (see, e.g., refs 12–14). The interpretation of the amorphous diffraction pattern is possible if the packing of neighboring molecules is modeled. For the amorphous phase of nylon 6, a two-dimensional pseudo-hexagonal close packing is usually assumed.⁵ The amorphous halo is then composed of reflections in the (100) range. The pole figure for the total amorphous halo intensity for the deformed compression-molded sample is presented in Figure 3e. It is seen that most of the (100) normals are oriented perpendicular to the drawing direction; i.e., the macromolecular chain axes are also mostly aligned along the drawing direction as might be expected. The pole figure of the amorphous halo width shown in Figure 5e demonstrates that the smallest peak width is for that large fraction of the amorphous phase that is oriented along the drawing direction [(100) normals perpendicular to the drawing direction].

Quite similar overall observations can be made with regard to the behavior of α and γ crystals in injection-molded nylon 6 samples during uniaxial deformation (pole figures in Figure 6 for peak intensity and those in Figure 7 are for peak width). The asymmetry resulting from the shape of the oarlike flat and wide tensile specimens is more pronounced for injection-molded samples. It should be noted here that the amount of higher modulus and higher yield stress γ phase¹⁵ is much larger in the injection-molded samples (28%) compared to the compression-molded samples (13%). It is the relative ease of plastic deformation of the more compliant α form (mainly by slip along and across the sheets of hydrogen bonds) which reduces the influence of the tensile specimen geometry in the course of deformation during drawing in compression-molded samples.

IV. Conclusions

The X-ray diffraction pattern of uniaxially deformed polyamide 6 shows a large overlapping of reflections from all crystalline forms and the amorphous phase. There is considerable advantage in deconvoluting these peaks in order to obtain information about each phase. The deconvolution procedure, based on a least-squares scheme, was applied here to obtain information about the orientation of crystalline entities in plastically deformed nylon 6 samples. Besides the total intensity pole figures, a new type of pole figure based on peak widths was proposed and proved to be of considerable importance in elucidating the mechanisms of plastic deformation of nylon 6 and giving useful information on crystallite size. Without the deconvolution procedure, pole figures based on as-received WAXS data lead to erroneous and confusing conclusions regarding crystallographic orientation in deformed nylon 6.

Plastic deformation of nylon 6 samples under uniaxial tension causes preferred orientation of the (200) direction of α -form crystals perpendicular to the orientation direction as the chain axes orient parallel to the drawing direction. The size of the crystals of the α form in the direction perpendicular to the (200) plane decreases slightly. The majority of α crystals are oriented with the (002) direction perpendicular to the deformation direction.

Normals for (0n0) crystallographic planes, parallel to macromolecular chains, of α and γ crystals are oriented parallel to the deformation direction.

As a result of plastic deformation there is a large amount of breakdown of α crystals particularly between (002) planes. It can be concluded that the most intense mechanism of deformation of α crystals of nylon 6 is slip along crystallographic planes containing hydrogen bonds (see Figure 4) and in the chain direction. Destruction of γ crystals of nylon 6 along a and c axes during plastic deformation occurs without any preference except for the influence of the initial shape of tensile specimens.

In compression-molded samples, where the α forms of crystals dominates, the orientation and deformation of the crystalline components are governed by the behavior of α crystals; the orientation and deformation of γ crystals is affected by the deformation of α crystals, indirectly. In injection-molded samples, where the content of γ crystals is relatively large, the orientation and deformation of the crystalline components during uniaxial drawing are governed more by the behavior of γ crystals; the orientation and deformation of α crystals is then affected by the deformation of γ crystals. The influence of the shape of tensile specimens on the course of deformation of injection-molded samples is more pronounced due to a larger concentration of the more rigid γ form¹⁵ compared to that of compression-molded nylon 6.

The amorphous phase becomes oriented mostly along the drawing direction and this fraction of the amorphous phase shows the smallest peak width.

Acknowledgment. This research conducted at M.I.T. has been supported in part by the NSF/MRL through the Center for Materials Science and Engineering at M.I.T., under Grant DMR-87-18718, and in part by DARPA under Contract (ONR) N00014-86-K-0768. The research in Lodz has been supported by CPBP 01.14 through the Polish Academy of Sciences.

References and Notes

- Cullity, B. D. *Elements of x-ray Diffraction*; Addison-Wesley Pub. Co.: Reading, MA, Menlo Park, CA, 1978, p 303.
- Rober, S.; Gehrhe, R.; Zachmann, H. G. *Mater. Res. Soc. Symp. Proc.* 1987, 79, 205.
- Galeski, A.; Argon, A. S.; Cohen, R. E. *Makromol. Chem.* 1987, 188, 1195.
- Galeski, A.; Argon, A. S.; Cohen, R. E. *Macromolecules* 1988, 21, 2761.
- Gurato, G.; Fichera, A.; Grandi, F. Z.; Zanetti, R.; Canal, P. *Makromol. Chem.* 1974, 175, 953.
- (a) Warren, B. E. *Phys. Rev.* 1941, 59, 693. (b) Kakudo, M.; Kasai, N. In *X-ray Diffraction by Polymers*; Kodansha, Ed.; Elsevier: Tokyo, Amsterdam, 1972; p 329.
- Holmes, D. R.; Bunn, C. W.; Smith, D. J. *J. Polym. Sci.* 1955, 17, 159.
- International Tables for X-Ray Crystallography*, III Kynoch Press: 1962; p 295.
- Peterlin, A. *Colloid Polym. Sci.* 1975, 253, 809.
- Peterlin, A. In *Polymeric Materials*; Baer, E., Ed.; American Society for Metals: Metals Park, OH, 1975; p 175.
- Peterlin, A. *J. Phys. Chem.* 1971, 75, 3921.
- Biagardi, H. J. *Makromol. Chem.* 1982, 183, 1785.
- Windle, A. H. In *Developments in Oriented Polymers*; Ward, I. M., Ed.; Elsevier: London, New York, 1986; Vol. 1, pp 1–46.
- Owens, A. J. In *Developments in Oriented Polymers*; Ward, I. M., Ed.; Elsevier: London, New York, 1987; Vol. 2, pp 237–268.
- Starkweather, H. M.; Moore, G. E.; Hansen, J. E.; Roder, T. M.; Brooks, R. E. *J. Polym. Sci.* 1985, 21, 189.